

KINETICS OF EVAPORATION AND DECOMPOSITION OF ISOPROPYL NITRATE BY RAPID SCAN IR SPECTROSCOPY

HORST KRAUSE, NORBERT EISENREICH and ACHIM PFEIL

Fraunhofer-Institut für Chemische Technologie, D-7507 Pfinztal (F.R.G.)

(Received 9 January 1989)

ABSTRACT

The evaporation and chemical decomposition kinetics of IPN were investigated at 200, 225 and 250 °C by monitoring the gas phase using rapid scan FTIR spectroscopy. Evaporation and decomposition rates were determined by a fit of a special model to the experimental absorption–time profiles. The model combines elements of the quasi-static theory and simple chemical reaction kinetics.

INTRODUCTION

The processes of most concern in the thermal analysis of liquids are evaporation and chemical decomposition. The analysis is difficult because of the interference between these events.

Evaporation and chemical decomposition are also the key processes in the combustion of liquid fuels, and parameters are sought to characterize these processes.

In this paper, the evaporation and chemical decomposition of the liquid fuel IPN (isopropyl nitrate) were investigated by monitoring the gas phase of the reacting sample. Rapid scan IR spectroscopy was employed to record absorption–time histories. These profiles were used to determine the evaporation rate and the chemical reaction rate by a least-squares fit of a combined evaporation and decomposition model.

THE MODEL

The pertinent parameters are the evaporation rate $K(T)$ and the chemical reaction rate $k(T)$. The model relates the rate parameters and the vapour mass m_v , the history of which is contained in the experimental absorption–time profiles.

The model assumes that evaporation and decomposition are consecutive processes and adopts the basic elements of the quasi-static theory [1].

Accordingly, a fuel droplet of a defined diameter is heated in the reaction cell set at the temperature T . On reaching the boiling point temperature T_v ($T_v \ll T$) the fuel evaporates, the vapour forming a radial flow pattern. On further heating the vapour attains the cell temperature T . At this temperature the vapour decomposes.

The vapour concentration is dependent on the decrease of the droplet mass and on the diameter of the spherical droplet. The dependence of the droplet diameter on time is described by

$$d^2 = d_0^2 - Kt \quad (1)$$

where d = droplet diameter, d_0 = initial droplet diameter, t = time and K = vaporisation rate.

Using eqn. (1), the decrease of the droplet mass with time is

$$dm/dt = -(3/2)K(m_0^{2/3}/d_0^2)m^{1/3} \quad (2)$$

where m = droplet mass and m_0 = initial droplet mass. The integral form of eqn. (2) is

$$m/m_0 = 2/3\{3/2[1 - (K/d_0^2)t]\}^{3/2} \quad (3)$$

The vapour mass is $m_v = (1 - m)$ and the vaporisation time is $t_v = d_0^2/K$.

For the chemical decomposition of m_v , a reaction order of 1 was assumed

$$dm_v/dt = -dm/dt - km_v \quad (4)$$

where k is the reaction rate constant. On combining eqns. (2), (3) and (4), the time history of m_v is obtained

$$m_v/m_0 = (3/2)^{7/6} K/d_0^2 \exp(-kt) \text{ integral } (1 - Kt/d_0^2)^{1/2} \exp(kt) dt \quad (5)$$

Assuming the Lambert-Beer law is obeyed, eqn. (5) corresponds to the experimental absorption-time profile because m_v is proportional to the vapour concentration.

Note the temperature dependence of K and k

$$K(T) = 8\beta/(c_p\$) \ln(1 + c_p(T - T_v)/L) \quad (6)$$

$$k(T) = z \exp(E_a/RT) \quad (7)$$

where β = thermal conductivity, $\$$ = density of the liquid, c_p = specific heat, T_v = boiling temperature, L = evaporation enthalpy, z = pre-exponential factor, E_a = activation energy and R = gas constant.

EXPERIMENTAL

Figure 1 depicts the reaction cell which withstands pressures up to 10 bar and can be set at a constant temperature ($\pm 1^\circ\text{C}$) in the interval 20–275°C.

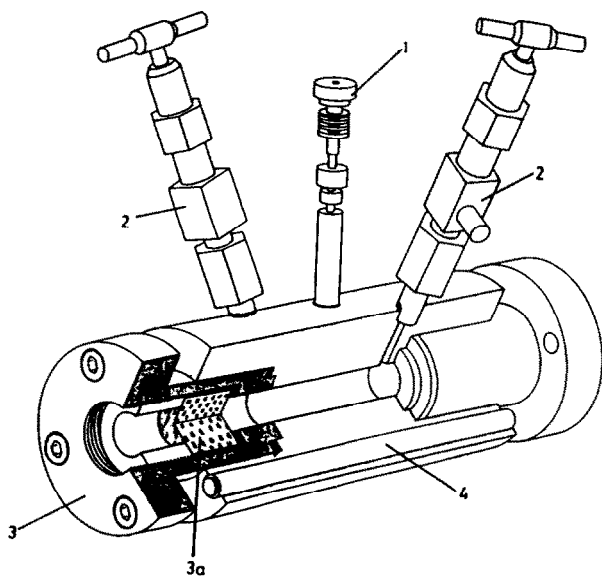


Fig. 1. Controlled heatable reaction cell: 1, septum-less injection system; 2, inlet/outlet valves; 3, flange; 3a, CaF_2 window; 4, heating rod of the cell housing.

The liquid is introduced into the chamber by a septum-less injection system (SGE OCI-3). The injected volume is variable between 0.2 and 10 μl . The cell volume is 8.9 cm^3 and the optical path length is 5.0 cm.

The cell is equipped with IR-transparent windows (CaF_2) in order to monitor the gas phase with the FT spectrometer (Nicolet 60 SX). The window diameter is 25 mm and the thickness is 15 mm. Kalrez standard 1050 was used to seal the windows to the cell body.

The gas phase was continuously inspected in the rapid scan mode (temporal resolution maximal 0.02 s, MCT detector). The absorption-time profiles were constructed from the recorded spectra by integrating the characteristic IR bands which are not overlapped by neighbouring bands.

For IPN, the nitrate symmetric stretching band centred at 1281 cm^{-1} [2] was selected and the boundaries for integration were set at 1279 and 1283 cm^{-1} . The temporal resolution used throughout the experiment was 0.25 s at a spectral resolution of 4 cm^{-1} (4096 data points). Less than 1 μl had to be injected in order to keep the absorbance of the gaseous IPN in the 0.1–1 range for the quantitative measurements.

The droplet diameter was determined by recording the injection process and the formation of the droplet in the gas phase of the cell using a video camera installed at the position of the IR spectrometer. The temporal resolution of the recording system was 0.04 ms and the temperature was varied from 150 to 250 $^\circ\text{C}$. The recordings showed that the symmetry of the droplets was spherical at temperatures above 150 $^\circ\text{C}$. The measured diameters ranged from 1.9 to 0.5 mm depending on the injected volume. The

formation of more than one droplet was avoided by injecting volumes measuring less than $0.5 \mu\text{l}$.

The injection volume used in all experiments was $0.2 \mu\text{l}$. The diameter of the droplet formed was $0.6 \pm 0.1 \text{ mm}$, on average.

IPN was purchased (Fluka purum 59640, density 1.04 g cm^{-3} , boiling point 102°C) and used without further purification.

RESULTS AND DISCUSSION

Isothermal runs were carried out at 200, 225 and 250°C . An example of the time histories obtained is shown in Fig. 2. The decreasing IPN absorption with time is marked by the bands at 1281 and 1647 cm^{-1} . The main products formed are formaldehyde and acetaldehyde at 1740 and 2740 cm^{-1} (the absorptions of the aldehydes overlap), nitromethane at 1573 cm^{-1} and CO_2 at 2339 cm^{-1} .

The corresponding concentration–time curves of IPN are depicted in Fig. 3, the symbols denoting the experimental values and the drawn lines delineating the fitted curves according to eqn. (5).

To calculate the curves, four fit parameters had to be used. The parameters are the rate constant $k(T)$, the vaporisation time $t_v = d_0^2/K(T)$, the delay time Δt between IPN injection and the onset of measurable evaporation and a scaling factor f_y to normalize the mass ratio. The values of the fit parameters are listed in Table 1.

The validity of the model is discussed by inspecting the $k(T)$ and $K(T)$ magnitudes. The latter are listed in Table 2 and are compared to evapora-

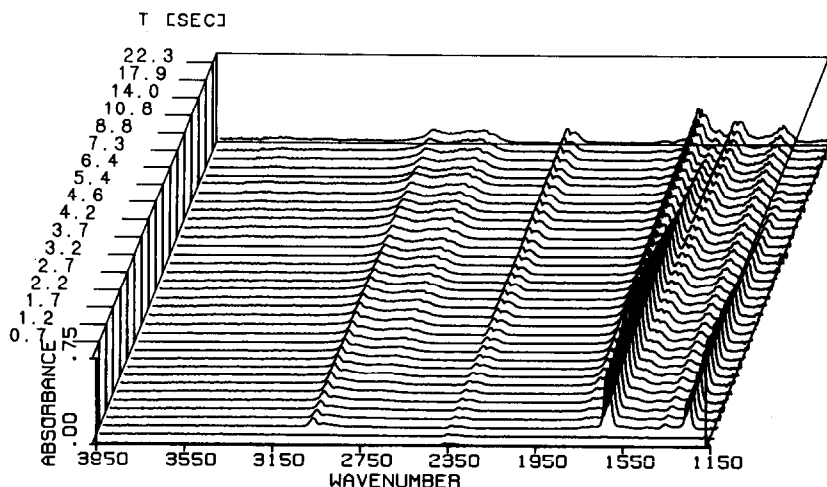


Fig. 2. Rapid scan IR absorption spectra of IPN evaporation and decomposition at 250°C .

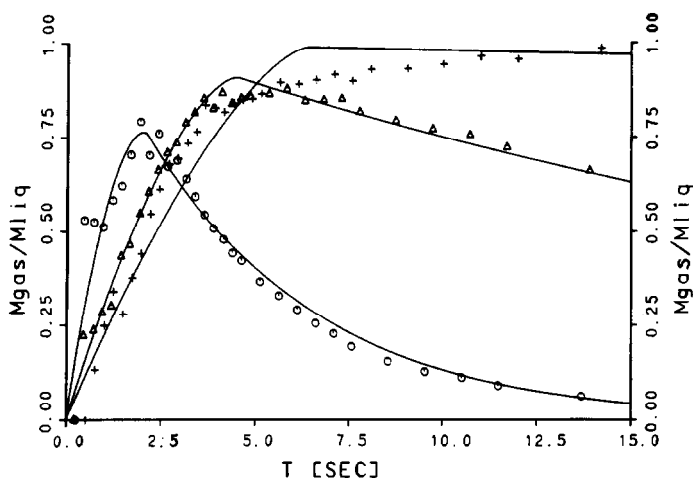


Fig. 3. Experimental (dotted lines) and calculated (drawn lines) concentration–time profiles of IPN at 200°C (+), 225°C (Δ) and 250°C (\odot).

tion rates which were calculated from experimental IPN parameters [3,4] by means of eqn. (6). With respect to the order of magnitude, both sets of rates are in accordance, which demonstrates the validity of the model.

Further support is provided by the chemical rates listed in Table 1 which are in order of magnitude accordance with the rates listed in Table 3. The latter were obtained from a first-order kinetic fit to the decaying part of the curves in Fig. 3 whereby evaporation was excluded. An example is shown in

TABLE 1

Fit parameters for IPN evaporation and decomposition

T (°C)	t_v (s)	$\log k$	f_y	Δt (s)
200	4.26	-2.6001	0.98	-0.28
225	3.03	-1.4564	1.13	0.04
250	1.43	-0.6537	1.26	0.24

TABLE 2

Evaporation parameters for IPN

T (°C)	t_v (s)	K_{exp}^a ($\text{mm}^2 \text{s}^{-1}$)	K_{theo} ($\text{mm}^2 \text{s}^{-1}$)
200	4.26	0.08	0.11
225	3.03	0.11	0.14
250	1.43	0.25	0.16

^a Droplet diameter 0.6 mm.

TABLE 3

Rate constants of IPN decomposition

$T(^{\circ}\text{C})$	$\log k(T)$				
175	-3.078	-3.025	-3.162	-3.246	-3.259
200	-2.321	-2.303	-2.298	-2.310	-2.314
225	-1.370	-1.370	-1.366	-1.406	-1.401
250	-0.537	-0.494	-0.535	-0.499	-0.554

Fig. 4 for the 200°C profile, the vertical line marking the onset of the fit. The curves were normalized and good fits were obtained as expressed by the low standard deviation of 2.5%.

This low deviation lent confidence to the use of the $k(T)$ values as a reference with which to inspect the rates in Table 1 more closely. They appear to be consistently somewhat lower, and led to a reconsideration of the models assumptions. It would appear that the IPN vapour must have partly decomposed before attaining the cell temperature T which is in contrast to what the model assumed. This discrepancy manifests itself in the apparent lower chemical rate constants.

To elucidate the IPN decomposition mechanism, profiles were constructed for the main products. Within the temporal resolution, the rise of the aldehydes and nitromethane absorption parallels that of the IPN decay, pointing to the O-NO₂ bond rupture as the rate-determining step. Furthermore, the activation energy to cleave this bond matches the bond energy. Depending on the environment, the nitrate bond energy is 150–175 kJ mol⁻¹ [5]. The Arrhenius plot of the rate constants is depicted in Fig. 5. The

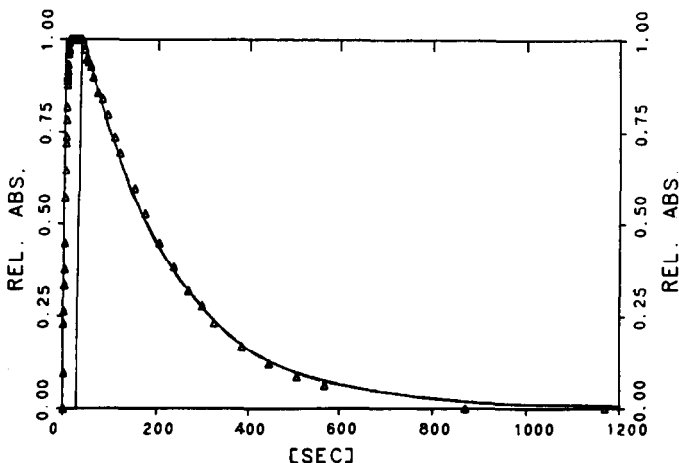


Fig. 4. First-order kinetic fit to the IPN absorption decay at 200°C.

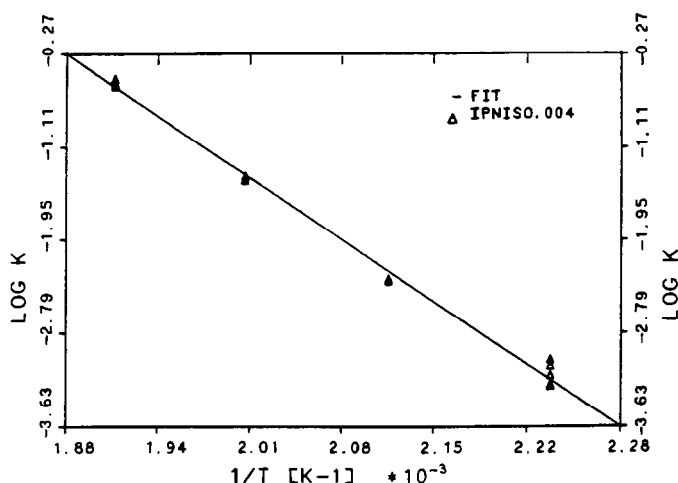


Fig. 5. Arrhenius plot of the IPN decomposition rate constants listed in Table 3.

resultant activation energy determined from the slope of the straight line is 158 kJ mol^{-1} and the frequency factor, $\log z$, is 15.2.

These values compare quite well with those obtained by Jullien et al. [6] in a shock tube experiment at $260\text{--}360^\circ\text{C}$, being $169.5 \text{ kJ mol}^{-1}$ and 16.5. Corresponding values for nitrate esters having a related structure are $154.5 \text{ kJ mol}^{-1}$ and 14.7 for *n*-propyl nitrate [7], and $154.5 \text{ kJ mol}^{-1}$ and 14.7 for ethyl nitrate [8].

CONCLUSION

A method is presented to determine the evaporation and chemical decomposition parameters of liquids. The experimental basis is a heated cell and a rapid scan IR spectrometer which monitors the gas phase. From the spectra which have subsecond temporal resolution, concentration–time profiles are constructed.

The profiles are complex because evaporation and chemical decomposition overlap. A special model is used to analyse the profiles. The model combines simple reaction kinetics and elements of the quasi-static theory and describes the evaporation of the droplet and the successive decomposition. The rates of both events are determined by a fit of the model to the experimental concentration–time curves.

The liquid fuel isopropyl nitrate (IPN) served as an example to test the model. The values determined for the temperature interval $200\text{--}250^\circ\text{C}$ ranged from 0.08 to $0.25 \text{ mm}^2 \text{ s}^{-1}$ for the evaporation rate and $-2.309\text{--}-0.523$ for the log of the chemical reaction rate. The order of magnitude of both rates matches those evaluated for IPN by different methods.

REFERENCES

- 1 F.A. Williams, *Combustion Theory*, Addison Wesley, Reading, MA, 1965.
- 2 R.A.G. Carrington, *Spectrochim. Acta*, 16 (1960) 1279.
- 3 G. Schmidt and A. Seidel, MBB Bericht UR-257-74 (1974), *Kurzzeit-Flüssigkeitsantrieb*.
- 4 M. Barrère and H. Moutet, *Tech. Aero.*, 9 (1956) 32.
- 5 J.F. Griffiths, M.F. Gilligan and P. Gray, *Combust. Flame*, 24 (1975) 11.
- 6 J. Jullien, J.-M. Pechine, F. Perez and M.A. Sadek, *Propellants, Explosives, Pyrotechnics*, 8 (1983) 99.
- 7 P. Gray, R. Shaw and J.C.J. Thynne, *Prog. Reaction Kinetics*, 4 (1967) 69.
- 8 F.H. Pollard, H.S.B. Marshall and A.E. Pedler, *Trans. Faraday Soc.*, 52 (1956) 59.